Volume 1 | Number 1 | Jan 2013 | Pages 1–100

ChemComm

Chemical Communications
www.rsc.org/chemcomm

ROYAL SOCIETY OF CHEMISTRY

This is an *Accepted Manuscript*, which has been through the Royal Society of Chemistry peer review process and has been accepted for publication.

Accepted Manuscripts are published online shortly after acceptance, before technical editing, formatting and proof reading. Using this free service, authors can make their results available to the community, in citable form, before we publish the edited article. We will replace this *Accepted Manuscript* with the edited and formatted *Advance Article* as soon as it is available.

You can find more information about *Accepted Manuscripts* in the **Information for Authors**.

Please note that technical editing may introduce minor changes to the text and/or graphics, which may alter content. The journal's standard **Terms & Conditions** and the **Ethical guidelines** still apply. In no event shall the Royal Society of Chemistry be held responsible for any errors or omissions in this *Accepted Manuscript* or any consequences arising from the use of any information it contains.

ChemComm

COMMUNICATION

Cluster-π electronic interaction in a superatomic Au₁₃ cluster bearing σ-bonded acetylide ligands†

Mizuho Sugiuchi,[a] Yukatsu Shichibu,[a,b] Takayuki Nakanishi,[c] Yasuchika Hasegawa [c] and Katsuaki Konishi [a,b,*]

An organometallic Au₁₃ cluster having two σ-bonded acetylide ligands was synthesized and its structure was determined by X-ray crystllography. Absorption spectral studies indicated the presence of the electronic coupling between the superatomic Au13 core and the acetylide π-orbitals, which was supported by theoretical considerations.

Gold-acetylide sigma bonds have been of general interest as they bring about the emergence of unique optical properties and reactive intermediates in catalysis.[1-9] For simple metal complexes, rich chemistry has been explored from both functional and structural perspectives. On the other hand, although numerous ligand-protected gold clusters have been synthesized,[10-14] examples of alkynyl-ligated clusters have been quite rare to date, and the nature of the bonding and electronic interaction between a cluster kernel and a C≡C π-system has not been experimentally characterized.[15-19] Tsukuda et al. have observed no appreciable electronic interaction in the optical absorption spectra of alkyne-protected gold clusters of diameter > 1 nm.[15,16] We have also demonstrated a similar phenomenon for a structurally precise Au₈ cluster with an anisotropic core+*exo*-type structure.[17] Herein we report the first experimental evidence of electronic interaction between a polyhedral gold core and a σ-bonded π-unit in the absorption spectrum of a phenylethynyl-modified Au₁₃ cluster with an icosahedral geometry and superatomic 8-electron system.[20-23] We have also investigated its electronic structure based on DFT calculations, which support the presence of electronic interaction between the superatomic gold core and π-conjugated units.

Regioselective introduction of two alkynyl ligands on the surface of the icosahedral Au₁₃ skeleton was achieved by the ligand-exchange reaction of a dichloro-substituted Au₁₃ cluster cation ([Au₁₃(dppe)₅Cl₂](PF₆)₃, **1**·(PF₆)₃), which was synthesized according to the HCl-mediated post-synthetic method.[21] The reaction cleanly proceeded by employing excess amounts of terminal alkynes and base (sodium methoxide), and the complete ligand exchange was verified by electrospray ionization mass spectrometry (ESI-MS) analysis of the reaction mixture. After workup, the crude product was recrystallized from acetonitrile and diethyl ether to give the pure dialkynyl-substituted cluster as its hexafluorophosphate salt ([Au₁₃(dppe)₅(C≡CPh)₂](PF₆)₃, **2**·(PF₆)₃), which was thoroughly characterized by ESI-MS analyses, elemental analyses, X-ray crystallography, and ^{1}H and ^{31}P NMR spectroscopies. For instance, the ESI mass spectrum of **2**·(PF₆)₃ showed a set of signals around *m/z* 1585, in perfect agreement with the calculated isotope pattern for [Au₁₃(dppe)₅(C≡CPh)₂]³⁺ (Fig. S2). Single-crystal X-ray analysis of **2**·(PF₆)₃ revealed that the cluster core adopts an icosahedral geometry. Two alkynyl ligands are σ-coordinated to the two diagonal apexes (Au1 and Au1′) of the icosahedron from the *trans* positions with Au–C perpendicular to the pentagon (Au2–Au6) of the icosahedron.

a. *Graduate School of Environmental Science, Hokkaido University, North 10 West 5, Sapporo 060-0810 Japan.*
  E-mail: konishi@ees.hokudai.ac.jp; Fax: +81 11 7064538; Tel: +81 11 7064538
b. *Faculty of Environmental Earth Science, Hokkaido University, North 10 West 5, Sapporo 060-0810 Japan.*
c. *Faculty of Engineering, Hokkaido University, North 13 West 8, Sapporo 060-8628 Japan.*

† Electronic Supplementary Information (ESI) available: Details of synthesis and crystal data of **2**•(PF₆)₃ (CCDC 1402657) and computational results of **1** and **2**. . For ESI and crystallographic data in CIF or other electronic format see DOI: 10.1039/x0xx00000x
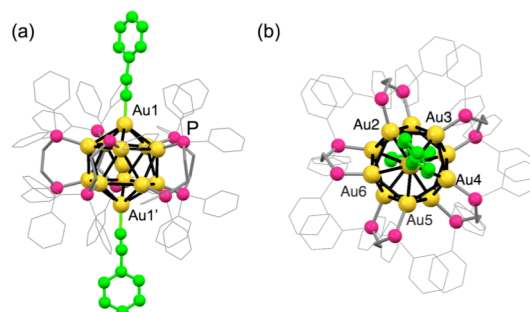

Fig. 1 (a) Side and (b) top views of the crystal structure of cationic moiety of **2**·(PF₆)₃. Phenylethynyl units (C≡CPh) are highlighted in light green and hydrogen atoms are omitted for clarity.

COMMUNICATION   **ChemComm**

Such σ-coordination of alkynyl ligands to the gold cluster surface is much different from the binding interface found in larger gold-alkynyl clusters synthesised by the reduction of gold(I) alkynyl precursors,[18,19] indicating the uniqueness of the post-synthetic ligand exchange method. The five diphosphine ligands (dppe) form a donut-like belt covering the rest of the surface of the icosahedron (Fig. 1b). These structural features are apparently similar to those observed for the precursor (**1**),[21] but there are slight differences that reflect the electron-withdrawing character of the anionic ligands. For the icosahedral core units, the bond lengths between the central and anion-bound apex gold atoms of **1** (2.696 and 2.697 Å) are appreciably shorter than those in **2** (2.757 Å). On the other hand, the distances from the central to the peripheral Au atoms in **1** and **2** are comparable (2.757–2.798 Å and 2.750–2.770 Å for **1** and **2**, respectively). However, the overall geometrical features and ligand-binding sites of the core were essentially preserved during the ligand-exchange reaction. The symmetrical structure of **2** in the solid state was maintained in solution without degradation or ligand migration, since only a single signal was observed in the ^{31}P NMR spectrum. Furthermore, the optical absorption spectrum of **2** in acetonitrile remained unchanged even after three weeks at room temperature (Fig. S3), implying its structural robustness.

As mentioned above, the two Au$_{13}$ clusters (**1** and **2**) have virtually identical icosahedral core structures. However, their optical absorption spectra in the visible region are different. As shown in Fig. 2, **1**·(PF$_6$)$_3$ in acetonitrile gave a single visible band at 495 nm (s1), whereas three bands were observed for the dialkynyl-substituted **2**·(PF$_6$)$_3$ (525, 488, and 438 nm; r1, r2, and r3). On the other hand, the UV absorption spectra were almost identical, featuring two bands at around 300 and 360 nm (inset). These observations indicate that the σ-bonded C≡CPh groups electronically affect the low-energy optical transitions that appear in the visible region.

To obtain further insights into the cluster-π interaction, we investigated the electronic structures of **1** and **2** in gas phase
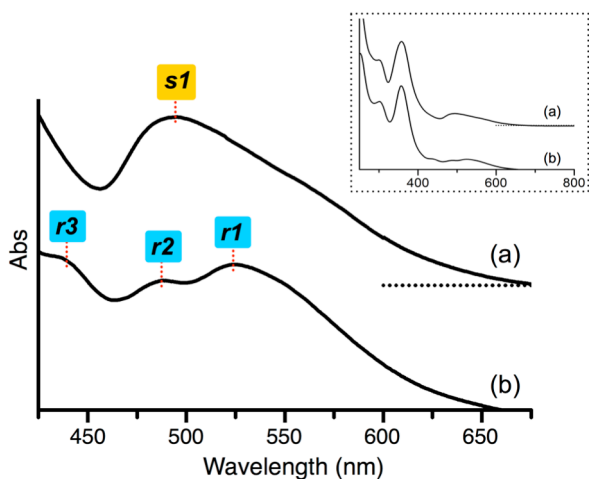

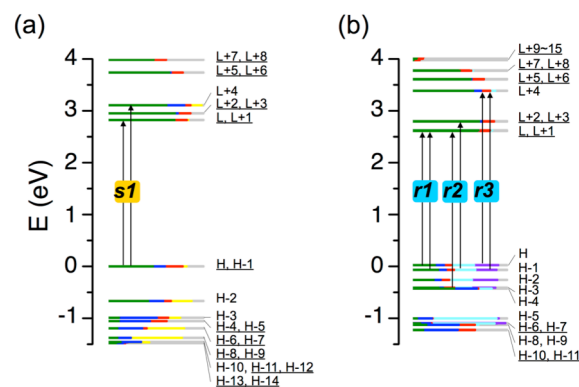
Fig. 3 Kohn-Sham (KS) orbital energy level diagrams of (a) 1 and (b) 2. Each KS orbital energy is relative to the HOMO energy and is drawn to indicate the relative contributions (line lengths with color labels) of the atomic orbitals of Au (6sp) in green, Au (5d) in blue, P (3p) in red, Cl (3p) in yellow, C (2p) for C≡C and Ph of C≡CPh units in light blue and violet, respectively, and miscellaneous in gray. H − X and L + Y represent HOMO − X and LUMO + Y, respectively. Underlines indicate the degeneracies of energy levels.

by DFT calculations, which have been widely used to study the electronic properties of related cluster compounds.[24-30] As shown in the Kohn−Sham energy diagrams (Fig. 3), marked differences were found between **1** and **2**, particularly in the occupied orbitals. For example, the electronic structure of **1** showed doubly degenerate HOMO/HOMO−1, which were fairly isolated from the closest occupied orbital (HOMO−2, ΔE ≈ 0.7 eV) (Fig. 3a). Atomic orbital composition analyses revealed that these orbitals as well as the unoccupied orbitals were preferentially composed of the Au(6sp) atomic orbitals (green lines), thus forming an sp-band (Table S3). On the other hand, the HOMO of **2** is accompanied by several energetically shallow occupied molecular orbitals (HOMO−1 to HOMO−4) at ΔE < −0.5 eV (Fig. 3b). Furthermore, substantial contributions from not only the gold atoms (green and blue) but also the π-conjugated units (C(2p), light-blue and violet) were observed in the HOMO and certain high-energy occupied orbitals (Table S5). This is in sharp contrast to the case of **1**, in which substantial contribution of the ligand (Cl) orbital was observed in the lower levels (e.g., HOMO−2). On the other hand, involvement of the π-orbitals was hardly observed in the unoccupied molecular orbitals of **2**. The LUMO and neighbouring orbitals were predominantly composed of the Au(6sp) atomic orbitals to constitute an sp-band, showing a similar feature to that observed for **1** (a). Thus, the attachment of the π-units to the Au$_{13}$ core causes appreciable perturbation on the occupied orbitals, giving rise to multiple cluster-π mixed states near the HOMO.

Based on the above findings, we conducted TD-DFT analyses to interpret the difference in the absorption spectra. As shown in Fig. S5, theoretical absorption spectra of **1** and **2** in gas phase were apparently in good agreement with the experimental results in acetonitrile, exhibiting large UV and small visible absorption bands. Cluster **1** showed critical involvements of HOMO→LUMO+1 and its degenerated

Fig. 2 Visible absorption spectra of (a) **1**·(PF$_6$)$_3$ and (b) **2**·(PF$_6$)$_3$ in MeCN at 25 °C. Inset shows the spectra over the whole measurement region.
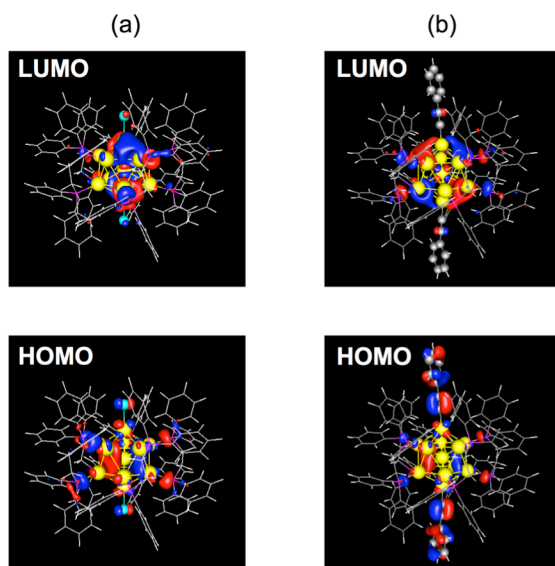
Fig. 4 HOMOs and LUMOs of (a) **1** and (b) **2**.

counterpart HOMO−1→LUMO for the lowest-energy transitions relevant to the visible absorption (Fig. 3a and Table S4). Since these orbitals constitute sp-bands, the visible band can be attributed to Au(6sp)→Au(6sp) intraband transitions, thus having the character of a metal-to-metal transition. Similarly, the HOMO and HOMO−1 of **2** served as principal ground states for the low-energy transitions, but as mentioned, the C(2p) π-orbitals from the C≡CC$_6$H$_5$ ligands substantially contributed to these orbitals. The HOMO→LUMO and HOMO−1→LUMO+1 transitions with high oscillator strengths gave smaller energies (2.23 eV) (Fig. 3b and Table S6) than the dominant low-energy transitions of **1** (2.34 eV) (Table S4), which is consistent with the presence of a red-shifted band in the experimental and simulated spectra (r1 in Fig. 2 and 3). Thus, the unique absorption spectral pattern of **2** (Fig. 2b) is unequivocally a result of the involvement of cluster-π mixed electronic states in the optical transitions. Fig. 4 depicts the spatial orbital distributions of the LUMOs and HOMOs of **1** and **2**. Cluster **1** showed superatomic D- and P-like molecular orbitals in the Au$_{13}$ core for the LUMO and HOMO, respectively (a), as expected from the delocalized electron model related to the 8-electron shell closure (1S^{2}1P^6 configuration).[25] Likewise, the LUMO of **2** showed D-like superatomic molecular orbitals (Fig. 4b, top). On the other hand, the HOMO of **2** was evidently extended over the C≡CC$_6$H$_5$ units from the Au$_{13}$ core (bottom), which is in accordance with the considerable participation of the C(2p) π-orbitals (Fig. 3b). In fact, orbital distributions over the π-units were also found in the other C(2p)-rich molecular orbitals, such as HOMO−1, HOMO−2, and HOMO−3 (Fig. S7). These occupied orbitals imparted the superatomic P-like character in the Au$_{13}$ core. Thus, interaction of the valence electrons of the gold superatom with the π-orbitals leads to the generation of unique molecular orbitals. This is the first example of the demonstration of electronic coupling between a superatom core and carbon-based π-systems.
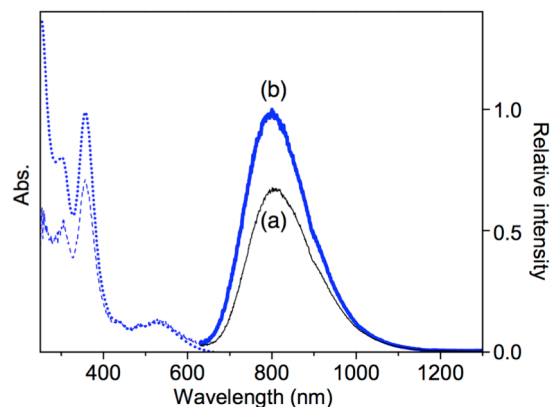

Fig. 5 Photoluminescence spectra of (a) **1**·(PF$_6$)$_3$ (λ_{ex} = 495 nm) and (b) **2**·(PF$_6$)$_3$ (λ_{ex} = 525 nm) in MeCN at 25 °C (absorbance at λ_{ex} = 0.1). Absorption (dotted) and excitation spectra (λ_{em} = 800 nm; dashed) of **2**·(PF$_6$)$_3$ are also provided for comparison.

Finally, we investigated the photoluminescence properties of the Au$_{13}$ clusters in acetonitrile at 25 °C. In the previous study, we reported that **1**·(PF$_6$)$_3$ exhibits a near-infrared emission upon excitation of the absorption band.[21,22] Photoluminescence with similar spectral shape and emission energy (approximately 800 nm) (Fig. 5) was shown by **2**·(PF$_6$)$_3$. The emissions of both clusters showed lifetimes on the order of microseconds (2.69 μs for **1** and 3.51 μs for **2**) and large Stokes shifts, indicating that they have phosphorescence character. On the other hand, the excitation spectra of **1**·(PF$_6$)$_3$ and **2**·(PF$_6$)$_3$ monitored at 800 nm are almost coincident with their absorption spectra (Fig. 5 and S4), so their excitation processes are different, as revealed in their electronic structures (Fig. 3). Therefore, the same emission spectral shapes and energies of **1** and **2** imply that the intermediate states responsible for the emissions (triplet or trap states) are virtually the same. The relative photoluminescence quantum yield of **2**·(PF$_6$)$_3$ (rhodamine 6G as standard) was estimated to be 0.16, which is appreciably greater than that of **1**·(PF$_6$)$_3$ (0.11, λ_{ex} = 495 nm), suggesting a quenching effect of the Cl atoms of **1**.

Herein we have experimentally demonstrated the presence of an electronic interaction of an 8-electron gold superatom with a σ-bonded π-system using a structurally defined alkynyl-substituted magic-number Au$_{13}$ cluster. The existence of the cluster-π electronic interaction was further supported by theoretical considerations. As a consequence of the steep progress in the structural chemistry of metal clusters, the versatility of the superatom concept for elucidating inherent stabilities, structures, and unusual properties has now been well established. Similar to conventional metal complexes, superatom complexes should be electronically stabilized by ligand binding, but the nature of the ligand−superatom interaction has not been clarified. In this respect, this study may provide impetus to further delineate the coordination chemistry of superatom complexes. Studies directed toward a deeper understanding of the ligand−superatom interaction coupled with the elaborate design of appropriate organic ligands are worthy

Chem. Commun.

of further investigation for the development of cluster-based functional materials.

Notes and references

‡ Crystallographic data for **2**•(PF$_6$)$_3$•4MeCN•2Et$_2$O: C$_{162}$H$_{162}$Au$_{13}$F$_{18}$N$_4$O$_2$P$_{13}$, M = 5502.12, monoclinic, a = 25.720(2) Å, b = 21.2708(18) Å, c = 31.007(3) Å, α = 90.00˚, β = 96.8650(9)˚, γ = 90.00˚, V = 16842(2) Å^3, T = 90 K, space group C2/c, Z = 4, 44566 reflections measured, 17155 independent reflections (R_{int} = 0.0662). The final R_1 value was 0.0651 ($I > 2\sigma(I)$). The final wR(F^2) values were 0.1924 ($I > 2\sigma(I)$). The final R_1 value was 0.1457 (all data). The final wR(F^2) value was 0.2604 (all data).

1. N. Long and C. Williams, *Angew. Chem. Int. Ed.*, 2003, **42**, 2586-2617.
2. J. Lima and L. Rodríguez, *Chem. Soc. Rev.*, 2011, **40**, 5442-5456.
3. C. Bronner and O. Wenger, *Dalton Trans.*, 2011, **40**, 12409-12420.
4. X. He and V. W.-W. Yam, *Coord. Chem. Rev.*, 2011, **255**, 2111-2123.
5. D. J. Gorin, B. D. Sherry and F. D. Toste, *Chem. Rev.*, 2008, **108**, 3351-3378.
6. A. Arcadi, *Chem. Rev.*, 2008, **108**, 3266-3325.
7. I. Braun, A. M. Asiri and A. S. K. Hashmi, *ACS Cat.*, 2013, **3**, 1902-1907.
8. V. Au, K. Wong, D. Tsang, M.-Y. Chan, N. Zhu and V. Yam, *J. Am. Chem. Soc.*, 2010, **132**, 14273-14278.
9. I. Koshevoy, Y.-C. Chang, A. Karttunen, S. Selivanov, J. Jänis, M. Haukka, T. Pakkanen, S. Tunik and P.-T. Chou, *Inorg. Chem.*, 2012, **51**, 7392-7403.
10. K. P. Hall and D. M. P. Mingos, *Prog. Inorg. Chem.*, 1984, **32**, 237-325.
11. T. Tsukuda, *Bull. Chem. Soc. Jpn.*, 2012, **85**, 151-168.
12. K. Konishi, *Struct. Bond.*, 2014, **161**, 49-86.
13. R. Jin, *Nanoscale*, 2015, **7**, 1549-1565.
14. D. M. P. Mingos, *Dalton Trans*, 2015, **44**, 6680-6695.
15. P. Maity, T. Wakabayashi, N. Ichikuni, H. Tsunoyama, S. Xie, M. Yamauchi and T. Tsukuda, *Chem. Commun.*, 2012, **48**, 6085-6087.
16. P. Maity, S. Takano, S. Yamazoe, T. Wakabayashi and T. Tsukuda, *J. Am. Chem. Soc.*, 2013, **135**, 9450-9457.
17. N. Kobayashi, Y. Kamei, Y. Shichibu and K. Konishi, *J. Am. Chem. Soc.*, 2013, **135**, 16078–16081.
18. X. K. Wan, S. F. Yuan, Q. Tang, D. E. Jiang and Q. M. Wang, *Angew. Chem. Int. Ed.*, 2015, **54**, 5977-5980.
19. X. K. Wan, Q. Tang, S. F. Yuan, D. E. Jiang and Q. M. Wang, *J. Am. Chem. Soc.*, 2015, **137**, 652-655.
20. C. E. Briant, B. R. C. Theobald, J. W. White, L. K. Bell, D. M. P. Mingos and A. J. Welch, *J. Chem. Soc., Chem. Commun.*, 1981, 201.
21. Y. Shichibu and K. Konishi, *Small*, 2010, **6**, 1216-1220.
22. Y. Shichibu, K. Suzuki and K. Konishi, *Nanoscale*, 2012, **4**, 4125-4129.
23. R. Dong, X. Chen, H. Zhao, X. Wang, H. Shu, Z. Ding and L. Wei, *Phys Chem Chem Phys*, 2011, **13**, 3274-3280.
24. J. Akola, M. Walter, R. L. Whetten, H. Häkkinen and H. Grönbeck, *J. Am. Chem. Soc.*, 2008, **130**, 3756-3757.
25. M. Walter, J. Akola, O. Lopez-Acevedo, P. D. Jadzinsky, G. Calero, C. J. Ackerson, R. L. Whetten, H. Grönbeck and H. Häkkinen, *Proc. Natl. Acad. Sci. USA*, 2008, **105**, 9157-9162.
26. M. Zhu, C. M. Aikens, F. J. Hollander, G. C. Schatz and R. Jin, *J. Am. Chem. Soc.*, 2008, **130**, 5883-5885.
27. Y. Kamei, Y. Shichibu and K. Konishi, *Angew. Chem. Int. Ed.*, 2011, **50**, 7442-7445.
28. Y. Shichibu, Y. Kamei and K. Konishi, *Chem. Commun.*, 2012, **48**, 7559-7561.
29. Y. Shichibu and K. Konishi, *Inorg. Chem.*, 2013, **52**, 6570-6575.
30. Y. Shichibu, M. Zhang, Y. Kamei and K. Konishi, *J. Am. Chem. Soc.*, 2014, **136**, 12892-12895.